

This is the accepted manuscript made available via CHORUS. The article has been published as:

# Is there a Difference in Van Der Waals Interactions between Rare Gas Atoms Adsorbed on Metallic and Semiconducting Single-Walled Carbon Nanotubes?

De-Li Chen, Lynn Mandeltort, Wissam A. Saidi, John T. Yates, Jr., Milton W. Cole, and J. Karl Johnson

Phys. Rev. Lett. **110**, 135503 — Published 26 March 2013

DOI: [10.1103/PhysRevLett.110.135503](https://doi.org/10.1103/PhysRevLett.110.135503)

# Is there a difference in van der Waals interactions between rare gas atoms adsorbed on metallic and semiconducting single walled carbon nanotubes?

De-Li Chen<sup>1</sup>, Lynn Mandeltort<sup>2</sup>, Wissam A. Saidi<sup>1</sup>, John T. Yates, Jr.<sup>2</sup>, Milton W. Cole<sup>3</sup>, and J. Karl Johnson<sup>1,4</sup>

<sup>1</sup>*Department of Chemical and Petroleum Engineering,  
University of Pittsburgh, Pittsburgh, PA, 15261, USA*

<sup>2</sup>*Department of Chemistry, University of Virginia, VA 22904, USA*

<sup>3</sup>*Department of Physics, Penn State University, University Park, PA 16802, USA and*

<sup>4</sup>*National Energy Technology Laboratory, Pittsburgh, PA 15236, USA*

Differences in polarizabilities of metallic (M) and semiconducting (S) single-walled carbon nanotubes (SWNTs) might give rise to differences in adsorption potentials. We show from experiments and van der Waals-corrected density functional theory (DFT) that binding energies of Xe adsorbed on M- and S-SWNTs are nearly identical. Temperature programmed desorption of Xe on purified M- and S-SWNTs give similar peak temperatures, indicating that desorption kinetics and binding energies are independent of the type of SWNT. Binding energies computed from vdW-corrected DFT are in good agreement with experiments.

PACS numbers: 61.48.De, 68.43.-h, 68.43.Vx, 73.22.-f

Multiwalled-carbon nanotubes were first identified in experiments by Iijima et al.<sup>1</sup> in 1991. Single-walled carbon nanotubes (SWNTs) were predicted theoretically<sup>2-4</sup> in 1992 and then experimentally observed in 1993.<sup>5,6</sup> SWNTs are either metallic (M-SWNT) or semiconducting (S-SWNT), depending on their chiral indices,  $(n, m)$ .<sup>4</sup> As a consequence of the symmetry of the SWNT, all nanotubes having  $n = m$  are metallic. When  $n - m$  is an integer multiple of 3 the SWNT will have a very small band gap, and SWNTs having all other chiral indices will be large gap semiconductors with band gaps inversely proportional to their radii.<sup>7,8</sup>

There are dramatic differences in the longitudinal polarizabilities of M- and S-SWNTs. Kozinsky et al.<sup>9</sup> predicted that the longitudinal polarizability of SWNTs scales as the inverse square of the band gap, so that M-SWNTs essentially have infinite static longitudinal polarizability. In contrast, the transverse polarizability of SWNTs is proportional to the square of the radius and independent of the band gap or chirality of the SWNT.<sup>9</sup> These theoretical predictions were confirmed experimentally by Lu et al.<sup>10</sup>

It has been widely assumed that the extraordinary differences in polarizabilities of M-SWNTs and S-SWNTs will lead to significant differences in the adsorption potentials and binding (adsorption) energies of weakly-bound adsorbates on SWNTs,<sup>11-14</sup> since conventional expressions for van der Waals (vdW) interaction coefficients are proportional to the polarizabilities of the interacting particles (or, equivalently, the dielectric functions of surfaces).<sup>15</sup> Unfortunately, there exists no rigorous expression for the vdW interaction energy between a SWNT (either metallic or semiconducting) and a physisorbed atom at its equilibrium separation. It is important to recognize that there are dramatic differences in the non-retarded *asymptotic* vdW energies for parallel metallic and semiconducting nanowires or nanotubes, as first noted by Chang et al.<sup>16</sup> and more recently by Dobson et al.,<sup>17</sup> but the extension to atoms interacting

with nanotubes at *equilibrium* distances has not yet been made. Perhaps the closest system with which we may compare is the expression for the vdW interaction of an atom with a semi-infinite solid, such as graphite. The potential for an adatom at a distance  $z$  from the surface can be expressed as<sup>18</sup>

$$V_{\text{vdW}}(z) = -C_3/z^3. \quad (1)$$

This equation is valid when  $z$  is large compared with the lattice constant of the substrate but small compared to the distance where retardation is important.  $C_3$  is the van der Waals constant, which can be approximated by<sup>18</sup>

$$C_3 = \frac{g_0 \alpha_0 E_a E_s}{8(E_a + E_s)}, \quad (2)$$

where  $\alpha_0$  and  $E_a$  are the static polarizability and excitation frequency of the adatom, and  $g_0$  and  $E_s$  are two substrate-dependent fitted parameters. The change in  $C_3$  as the substrate is changed from semiconducting to metallic can be approximated by assuming the contribution is additive:

$$\frac{\Delta C_3}{C_3} = \frac{\hbar \omega_{sp}(E_a + E_s)}{g_0 E_s (E_a + \hbar \omega_{sp})}, \quad (3)$$

where  $\omega_{sp}$  is the surface plasma frequency of the free electrons,<sup>19</sup>

$$\omega_{sp}^2 = \frac{2\pi n e^2}{m_e}. \quad (4)$$

Here,  $n$  is the density of free electrons,  $e$  is the charge on an electron, and  $m_e$  is the effective mass of an electron. We see that  $\Delta C_3$  is proportional to the square root of the density of free electrons, indicating a possible weak response to the change from semiconducting to metallic SWNTs. Values of  $E_a$  for Xe and  $g_0$ ,  $E_s$  for graphite are available.<sup>18</sup> The value of  $n$  is the only unknown, and unfortunately is difficult to estimate. We can, however

get a rough estimate of the magnitude of  $\Delta C_3/C_3$  by specifying a value of  $\hbar\omega_{sp}/E_s$  in Eq. (3) and assuming that  $E_a \gg \hbar\omega_{sp}$ . Specifying  $\hbar\omega_{sp}/E_s = 0.01$ , which is meant to mimic the injection of a small number of electrons, we get  $\Delta C_3/C_3 = 0.04$  for the Xe/graphite system. This indicates that the vdW potential may increase significantly as the substrate changes from semiconducting to metallic. However, there are problems with this approach. The half-space solution presented above is not applicable to nanotubes, which have only a single layer of atoms and therefore lack complete screening.<sup>17</sup> In addition, The metallic behavior of nanotubes is confined to the longitudinal direction. Thus, although the preceding heuristic argument suggests that a small number of conducting electrons has a modest effect on the vdW interaction, there is no rigorous theoretical answer to the question posed here.

The question has also been difficult to resolve from accurate numerical quantum mechanical calculations. The difficulty in answering the question from quantum mechanics comes from the approximate nature of the methods one must use to compute the interaction between an adsorbate and a SWNT. Density functional theory (DFT) with conventional local and semilocal functionals does not capture nonlocal electron correlation effects for small electron density overlap and therefore cannot be used to compute long-range vdW interactions accurately.<sup>20</sup> Møller-Plesset perturbation theory, which does capture much of the dispersion interaction, diverges for metallic systems,<sup>21,22</sup> and therefore cannot be used to compute interaction energies for atoms with M-SWNTs. Quantum Monte Carlo (QMC) methods could provide accurate binding energies but these methods are computationally very expensive and are challenging to implement for metallic systems.<sup>23</sup> Another approach is to compute the correlation energy from the random phase approximation (RPA), combined with exact Hartree-Fock exchange energy. However, this approach also carries a very steep computational cost.<sup>24,25</sup> Recently developed methods to include vdW interactions within DFT, such as the second-generation van der Waals density functional theory (vdW-DF2) of Langreth and coworkers,<sup>26</sup> provide a compromise between accuracy and efficiency. Although these methods do not include true many-body effects, it has been shown that they give binding energies in excellent agreement with QMC and RPA calculations for water on graphene.<sup>27</sup>

It has also been impossible to experimentally address the question of adsorbate interactions with M- and S-SWNTs until very recently. This is because all current synthesis methods produce mixtures of M- and S-SWNTs and there has not been an efficient way to separate them in sufficiently large quantities until the work of Hersam et al., who used density differentiation to separate M- and S-SWNTs.<sup>28,29</sup>

We present a combined theoretical and experimental approach to answer the question of whether the binding energy of Xe to M-SWNTs is significantly different

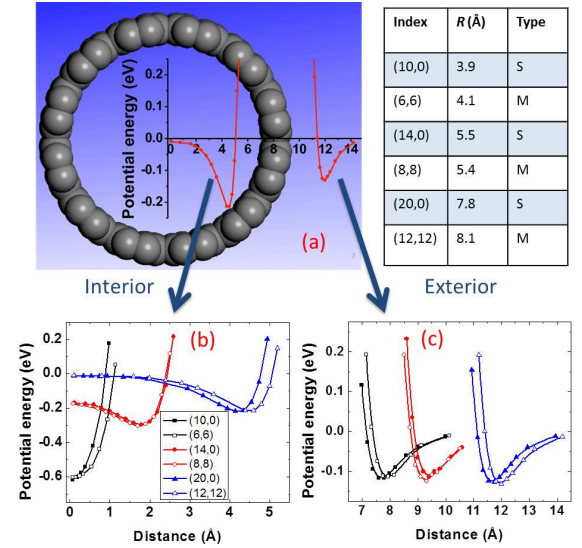


FIG. 1. (color online) (a) Schematic of the potential energy curves for Xe on the inside and outside of a (12,12) SWNT as a function of distance from the center of the SWNT. Potential energy curves for (b) interior and (c) exterior adsorption of Xe on a series of M- and S-SWNTs. The chiral index, radius ( $R$ ) and the type of each of the SWNTs are shown in the inset table.

from binding to S-SWNTs. We use vdW-DF2 in our calculations. This method has been shown to be accurate for predicting the energetics of rare gas atoms on metal surfaces.<sup>20,30</sup> We also use the method of Tkatchenko and Scheffler<sup>31</sup> (vdW-TS) as an independent test of the vdW-DF2 approach. We experimentally probe the kinetics and energetics of Xe binding to M- and S-SWNTs by employing temperature programmed desorption (TPD) of Xe on purified samples of either M- or S-SWNTs.

We have computed potential energy curves for Xe adsorption on the inside and outside [Fig. 1(a)] of six different nanotubes, three metallic and three semiconducting.<sup>32</sup> The nanotubes are divided into three sets, with each set having one M-SWNT and one S-SWNT of nearly identical diameters. The chiral index, radius and type of each nanotube are given in Fig. 1. We have computed the potential energy, defined as

$$E_{\text{pot}} = E_{\text{tot}} - E_{\text{Xe}} - E_{\text{SWNT}}, \quad (5)$$

where  $E_{\text{tot}}$  is the DFT energy of the Xe/SWNT system,  $E_{\text{Xe}}$  is the energy of an isolated Xe atom, and  $E_{\text{SWNT}}$  is the energy of an isolated SWNT. The potential energy curves for Xe approaching the center of a carbon hexagon for six different SWNTs computed from vdW-DF2 are plotted in Figs. 1(b) and (c).

We see that the predictions from our vdW-DF2 calculations indicate that there is little difference between the potential energy curves for Xe on M-SWNTs and S-SWNTs; the differences in the repulsive parts of the potential energy curves shown in Fig. 1 can be attributed to slight differences in the diameters of the SWNTs. Specif-

ically, the (10,0) tube is 0.2 Å smaller in radius than the (6,6) tube, which corresponds closely to the distance between the repulsive parts of the potentials for these two tubes in Fig. 1 (b) and (c). The same trends can be observed for the other two pairs of tubes. Hence, the potential energy curves depend critically on the diameter of the SWNT, but not significantly on the electronic properties of the SWNT. The largest difference in the well depths for a given pair of SWNTs (having similar diameters) is about 0.02 eV. The binding energy is larger in magnitude for endohedral than exohedral adsorption, as has been known to be the case from previous experiments<sup>33</sup> and theory.<sup>34</sup>

We have performed TPD experiments on purified samples of either S-SWNTs or M-SWNTs. The S- and M-SWNT samples used in this study are commercial samples prepared by arc discharge and separated using proprietary surfactants and density gradient centrifugation.<sup>28</sup> The average diameters for both S- and M-SWNTs are essentially identical with a value of about 1.4 nm, so that we can compare the adsorption strength of Xe on S- and M-SWNTs without a bias due to differences in curvature of the nanotubes. As shown in Fig. 2 (a)-(b), three different adsorption experiments (labeled as 1, 2, and 3 on both S- and M-SWNT) were performed independently to compare the Xe desorption kinetics, where the initial coverage of Xe on S- and M-SWNTs in each of the three experiments is the same. The value of  $T_{\text{peak}}$  corresponds to the maximum rate of desorption and therefore is used to compare Xe desorption on the two samples. The  $T_{\text{peak}}$  values are used to estimate the desorption energies through the Redhead equation<sup>35</sup> using a typical preexponential factor for the first-order desorption process of  $\nu = 10^{12} \text{ s}^{-1}$  and our heating rate of  $2 \text{ K s}^{-1}$ . The peak temperatures as well as the estimated desorption energies based on the three experiments are listed in Table I.<sup>36</sup> These values are essentially identical with energy differences less than 0.01 eV. We note that at the low coverages in the experiments essentially all the gas will be adsorbed on the endohedral sites.<sup>33</sup> Our experimental results are in excellent agreement with predictions from our vdW-DF2 calculations, shown in Table II, which also show a very slight difference between S- and M-SWNTs of similar diameters. Moreover, the values of the experimentally determined desorption energies are in good agreement with the absolute values of the calculated adsorption energies. Our computed binding energies on tubes having diameters of about 16 Å and 11 Å are about -0.22 eV and -0.30 eV, respectively. This range of values is in good quantitative agreement with the experimentally measured desorption energy of about 0.33 eV. Note that the experimental SWNT samples have a range of diameters with a mean value of about 14 Å.

We have computed the potential energy curves for Xe on the exterior of (12,12) and (20,0) SWNTs using the vdW-TS method<sup>31</sup> as an independent check of our vdW-DF2 calculations. These curves are plotted in Fig. 3, along with results from the Perdew-Burke-Ernzerhof

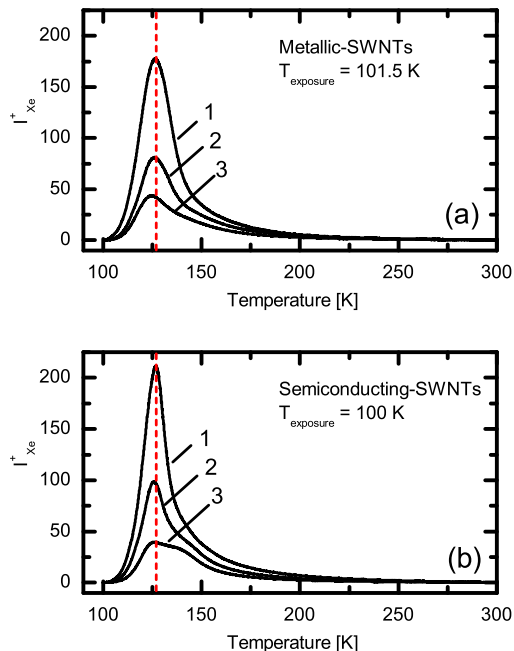


FIG. 2. Temperature programmed desorption spectra of Xe desorbing from (a) M-SWNTs and (b) S-SWNTs. The coverage of Xe, as measured by the area under the curve, is the same for the curves having the same label; e.g., curve 1 in (a) has the same coverage of Xe as curve 1 in (b). The heating rate is  $dT/dt = 2 \text{ K s}^{-1}$ . Vertical lines are guides to the eye.

TABLE I. (color online) Comparison of measured Xe desorption energies,  $E_{\text{des}}$  (in eV), for S- and M-SWNTs from three independent experiments. The TPD peak temperatures (in K) are given in parentheses.

Expt.	S-SWNTs, ( $T_{\text{peak}}$ )	M-SWNTs, ( $T_{\text{peak}}$ )
1	0.34 (127.2)	0.33 (126.4)
2	0.33 (126.1)	0.33 (127.1)
3	0.33 (125.6)	0.33 (125.5)

(PBE) generalized gradient approximation functional,<sup>37</sup> the local density approximation (LDA),<sup>38</sup> and empirical Lennard-Jones (LJ) potential calculations. We used the standard LJ parameters for carbon in graphite<sup>39,40</sup> and Xe-Xe LJ parameters from the literature.<sup>41,42</sup> Lorentz-Berthelot combining rules were used to compute the Xe-C cross interactions. We see that the vdW-TS calculations agree with the vdW-DF2 results very well over the range of distances covered. In contrast to these two functionals, PBE shows essentially no binding, as is the case for PBE calculations of Xe adsorption on various metal surfaces.<sup>20,30</sup> The LDA calculations underestimate both the equilibrium distance and the potential well depth. It is interesting that the LJ potential energy curves are in

TABLE II. The vdW-DF2 calculated desorption energies (negative of adsorption energy, in eV) of Xe on interior (exterior) sites of M-SWNTs and S-SWNTs.

M-SWNT	$E_{\text{des}}$	S-SWNT	$E_{\text{des}}$
(6,6)	0.60 (0.12)	(10,0)	0.62 (0.12)
(8,8)	0.30 (0.13)	(14,0)	0.30 (0.12)
(12,12)	0.22 (0.13)	(20,0)	0.22 (0.13)

rather good agreement with those computed from vdW-DF2 and vdW-TS, having similar equilibrium distances and slightly less attractive (by about 0.01 eV) adsorption energies. Thus, the empirical LJ potential, which is derived from simple combining rules using pure fluid data for Xe and carbon parameters for graphite, provides a reasonably good estimate of the potential energy for Xe on SWNTs. We speculate that the potential energies of other rare gas atoms adsorbed on SWNTs will also show similar agreement between vdW-DF2, vdW-TS, and LJ potential calculations.

As a further check on the accuracy of our DFT methods we have computed the binding energy of He and Xe on graphite, for which reliable experimental data are available. We computed a well depth for He/graphite (hollow site) of 0.034 and 0.040 eV from vdW-DF2 and vdW-TS, respectively. The well depth computed from a potential derived from experiments (taking into account quantum effects) is about 0.019 eV.<sup>43</sup> Our computed binding energy is about a factor of 2 larger in magnitude than the experimentally-derived value. While this is a very large relative error, the absolute error is only about 0.02 eV, which is better than one might expect from DFT calculations. Our Xe/graphite (hollow site) results give binding energies of  $-0.17$  and  $-0.18$  eV from vdW-DF2 and vdW-TS, respectively, in good agreement with experimental values, which fall in the range of about  $-0.16$  to  $-0.17$  eV.<sup>44</sup> To the best of our knowledge, these are the first reported results for periodic plane wave vdW-corrected DFT calculations on the He/graphite and Xe/graphite systems. The good agreement between our calculations and experiments indicates that our calculations should be reasonably accurate for Xe/SWNT interactions.

In summary, we have found from both experiments and vdW-corrected DFT calculations that there are very small differences in the binding energies between Xe and either S- or M-SWNTs. These results are expected to apply to all cases where the interaction potential between an adsorbate molecule and a SWNTs is dominated by weak vdW interactions. This paper has encouraging implications concerning modern methods of computing vdW interactions within DFT, which have been found here to be fully consistent with our desorption experiments. The success of the simple LJ potential implies that interactions deduced from the very abundant data for physisorption of molecules on graphite can be transferred to these same molecules interacting

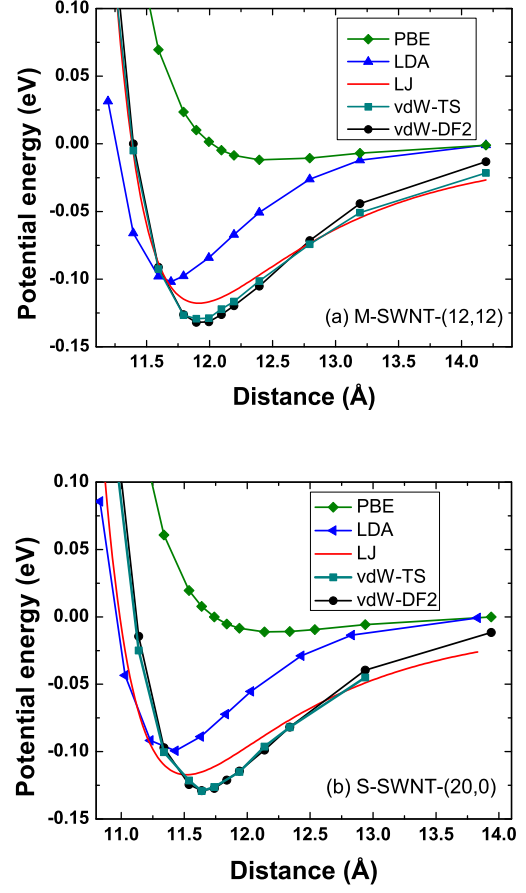


FIG. 3. (color online) Potential energy curves for Xe on the exterior of (a) a (12,12) M-SWNT and (b) a (20,0) S-SWNT as computed from PBE (green diamonds), LDA (blue triangles), Lennard-Jones potential (red line), vdW-TS (cyan squares), and vdW-DF2 (black circles).

with SWNTs. Our findings can be rationalized in two ways:<sup>45</sup> (1) Point-like objects like atoms do not strongly excite the long-wavelength electron density fluctuations that give rise to the unconventional vdW interactions between M-SWNTs at asymptotically large distances.<sup>16,17</sup> (2) The gapless  $\pi_z \rightarrow \pi_z^*$  transitions in M-SWNTs that give rise to anomalous interactions that are negligible close to the potential minimum.<sup>46</sup> Hence, our findings will likely not hold for highly polar and large molecules, such as surfactants,<sup>28,29</sup> and will not be accurate for computing interactions at asymptotically large distances.

## ACKNOWLEDGMENTS

We thank John Dobson and Gerald Mahan for helpful discussions. Funding was provided by the U.S. Department of Energy for funding under grant number DE-FG02-10ER16165 and by DTRA under contract HDTRA1-09-1-0008. Calculations were performed at the



- <sup>1</sup> S. Iijima, *Nature* **354**, 56 (1991).
- <sup>2</sup> M. S. Dresselhaus, G. Dresselhaus, and R. Saito, *Phys. Rev. B* **45**, 6234 (1992).
- <sup>3</sup> J. W. Mintmire, B. I. Dunlap, and C. T. White, *Phys. Rev. Lett.* **68**, 631 (1992).
- <sup>4</sup> N. Hamada, S.-i. Sawada, and A. Oshiyama, *Phys. Rev. Lett.* **68**, 1579 (1992).
- <sup>5</sup> S. Iijima and T. Ichihashi, *Nature* **363**, 603 (1993).
- <sup>6</sup> D. S. Bethune, C. H. Kiang, M. S. Devries, G. Gorman, R. Savoy, J. Vazquez, and R. Beyers, *Nature* **363**, 605 (1993).
- <sup>7</sup> S. G. Louie, in *Carbon Nanotubes Synthesis, Structure, Properties, and Applications*, edited by M. S. Dresselhaus, G. Dresselhaus, and P. Avouris (Springer-Verlag, Berlin, 2001), pp. 113–145.
- <sup>8</sup> J.-C. Charlier, X. Blase, and S. Roche, *Rev. Mod. Phys.* **79**, 677 (2007).
- <sup>9</sup> B. Kozinsky and N. Marzari, *Phys. Rev. Lett.* **96**, 166801 (2006).
- <sup>10</sup> W. Lu, D. Wang, and L. Chen, *Nano Lett.* **7**, 2729 (2007).
- <sup>11</sup> D. Chattopadhyay, I. Galeska, and F. Papadimitrakopoulos, *J. Am. Chem. Soc.* **125**, 3370 (2003).
- <sup>12</sup> M. Zheng, A. Jagota, E. D. Semke, B. A. Diner, R. S. M. S. R. Lustig, R. E. Richardson, and N. G. Tassi, *Nat. Mater.* **2**, 338 (2003).
- <sup>13</sup> P. Anilkumar, K. A. S. Fernando, L. Cao, F. Lu, F. Y. W. Song, S. Sahu, H. Qian, T. J. Thorne, A. Anderson, and Y.-P. Sun, *J. Phys. Chem. C* **115**, 11010 (2011).
- <sup>14</sup> J. Lu, S. Nagase, X. Zhang, D. Wang, M. Ni, Y. Maeda, T. Wakahara, T. Nakahodo, T. Tsuchiya, T. Akasaka, Z. Gao, D. Yu, H. Ye, W. N. Mei, and Y. Zhou, *J. Am. Chem. Soc.* **128**, 5114 (2006).
- <sup>15</sup> See Eq. (2) or the analogous equation of London for the coefficient  $C_6$  of the interatomic interaction.
- <sup>16</sup> D. B. Chang, R. L. Cooper, J. E. Drummond, and A. C. Young, *Phys. Lett.* **37A**, 311 (1971).
- <sup>17</sup> J. F. Dobson, A. White, and A. Rubio, *Phys. Rev. Lett.* **96**, 073201 (2006).
- <sup>18</sup> L. W. Bruch, M. W. Cole, and E. Zaremba, *Physical Adsorption: Processes and Phenomena* (Oxford University Press Inc., New York, 1997).
- <sup>19</sup>  $\omega_{sp} = \omega_p/\sqrt{2}$ , where  $\omega_p$  is the plasma frequency.
- <sup>20</sup> D.-L. Chen, W. A. Al-Saidi, and J. K. Johnson, *Phys. Rev. B* **84**, 241405(R) (2011).
- <sup>21</sup> A. Grüneis, M. Marsman, and G. Kresse, *J. Chem. Phys.* **133**, 074107 (2010).
- <sup>22</sup> M. Gell-Mann and K. A. Brueckner, *Phys. Rev.* **106**, 364 (1957).
- <sup>23</sup> W. M. C. Foulkes, L. Mitas, R. J. Needs, and G. Rajagopal, *Rev. Mod. Phys.* **73**, 33 (2001).
- <sup>24</sup> S. Lebègue, J. Harl, T. Gould, J. G. Ángyán, G. Kresse, and J. F. Dobson, *Phys. Rev. Lett.* **105**, 196401 (2010).
- <sup>25</sup> T. Olsen, J. Yan, J. J. Mortensen, and K. S. Thygesen, *Phys. Rev. Lett.* **107**, 156401 (2011).
- <sup>26</sup> K. Lee, É. D. Murray, L. Kong, B. I. Lundqvist, and D. C. Langreth, *Phys. Rev. B* **82**, 081101 (2010).
- <sup>27</sup> J. Ma, A. Michaelides, D. Alfè, L. Schimka, G. Kresse, and E. Wang, *Phys. Rev. B* **84**, 033402 (2011).
- <sup>28</sup> M. S. Arnold, A. A. Green, J. F. Hulvat, S. I. Stupp, and M. C. Hersam, *Nat. Nano.* **1**, 60 (2006).
- <sup>29</sup> A. L. Antaris, J. W. T. Seo, A. A. Green, and M. C. Hersam, *ACS Nano* **4**, 4725 (2010).
- <sup>30</sup> D.-L. Chen, W. A. Al-Saidi, and J. K. Johnson, *J. Phys.: Condens. Matter* **24**, 424211 (2012).
- <sup>31</sup> A. Tkatchenko and M. Scheffler, *Phys. Rev. Lett.* **102**, 073005 (2009).
- <sup>32</sup> Calculation details: Periodic plane wave DFT calculations were performed with the Vienna ab initio Simulation Package (VASP).<sup>47–50</sup> The vdW-TS approach, developed by Tkatchenko and Scheffler,<sup>31</sup> was implemented into a modified version of VASP by Al-Saidi et al.<sup>51</sup> The SWNT calculations employed large orthorhombic supercells with vacuum spacing of at least 15 Å in the directions perpendicular to the tube axis to mitigate the interactions between the periodic images. The direction parallel to the tube axis consisted of either 2 (8.52 Å) or 3 (7.38 Å) primitive unit cells for S- and M-SWNTs, respectively. This ensured that the Xe-Xe interactions were less than 2 meV. The Brillouin zone for SWNT calculations was sampled using a Monkhorst-Pack<sup>52</sup>  $1 \times 1 \times 3$  grid. The graphite calculations utilized a hexagonal supercell containing two layers of graphene, each having 32 carbon atoms. The cell dimensions were  $9.83 \times 9.83 \times 18.26$  Å. The periodic Xe-Xe interaction in this cell was found to be about 3 meV. The Brillouin zone was sampled with a  $7 \times 7 \times 1$  grid. A planewave energy cutoff of 600 eV was used for all the calculations.
- <sup>33</sup> P. Kondratyuk and J. T. Yates, Jr., *Acc. Chem. Res.* **40**, 995 (2007).
- <sup>34</sup> G. Stan and M. W. Cole, *Surf. Sci.* **395**, 280 (1998).
- <sup>35</sup> P. A. Redhead, *Vacuum* **12**, 203 (1962).
- <sup>36</sup> A small temperature offset of  $\delta T = 1.5$  K was uniformly applied to the temperature scale for the M-SWNTs in order to correct for the temperature differences between the S- and M-SWNT samples. The temperature scales on the two sample holders were calibrated by using the desorption kinetics of multilayer n-heptane from the Au plates as an independent thermometer to establish the magnitude and reproducibility of temperature scale differences on the two sample holders.
- <sup>37</sup> J. P. Perdew, K. Burke, and M. Ernzerhof, *Phys. Rev. Lett.* **77**, 3865 (1996).
- <sup>38</sup> J. P. Perdew and A. Zunger, *Phys. Rev. B* **23**, 5048 (1981).
- <sup>39</sup> W. A. Steele, *Surf. Sci.* **36**, 317 (1973).
- <sup>40</sup>  $\epsilon_{C-C}/k_B = 28$  K and  $\sigma_{C-C} = 3.4$  Å, where  $\epsilon$  is the potential well depth,  $k_B$  is the Boltzmann constant, and  $\sigma$  is the atomic diameter.
- <sup>41</sup> M. R. LaBrosse and J. K. Johnson, *J. Phys. Chem. C* **114**, 7602 (2010).
- <sup>42</sup>  $\epsilon_{Xe-Xe}/k_B = 221$  K and  $\sigma_{Xe-Xe} = 4.1$  Å.
- <sup>43</sup> W. E. Carlos and M. W. Cole, *Surf. Sci.* **91**, 339 (1980).
- <sup>44</sup> G. Vidali, G. Ihm, H.-Y. Kim, and M. W. Cole, *Surf. Sci. Rep.* **12**, 135 (1991).
- <sup>45</sup> Private communication from John F. Dobson.
- <sup>46</sup> J. F. Dobson and G. Tim, *J. Phys.: Condens. Matter* **24**, 073201 (2012).
- <sup>47</sup> G. Kresse and J. Hafner, *Phys. Rev. B* **47**, 558 (1993).

- <sup>48</sup> G. Kresse and J. Hafner, Phys. Rev. B **49**, 14251 (1994).
- <sup>49</sup> G. Kresse and J. Furthmuller, Phys. Rev. B **54**, 11169 (1996).
- <sup>50</sup> G. Kresse and J. Furthmuller, Comput. Mater. Sci. **6**, 15 (1996).
- <sup>51</sup> W. A. Al-Saidi, V. K. Voora, and K. D. Jordan, J. Chem. Theory Comput. **8**, 1503 (2012).
- <sup>52</sup> H. J. Monkhorst and J. D. Pack, Phys. Rev. B **13**, 5188 (1976).